

Characteristics of Asymmetric Ring Heads

Chia Shen Wang (王嘉申) and Huei Li Huang (黃暉理)

*Department of Physics, National Taiwan University,
Taipei, Taiwan*

(Received October 21, 1988)

The head field distribution of asymmetric ring heads with several inclination angles has been calculated. Both the H_x and H_y components of the field at large angles of inclination and low spacings exhibit good behaviour which can be beneficially exploited to improve the halfwidth and the peak level of the signal. These and other characteristic features and the potential applications to longitudinal and perpendicular recording are discussed.

I. INTRODUCTION

A high density of bits is a key concern in the development of digital computers. The theoretical and experimental studies of both longitudinal and vertical modes of magnetic recording all support the idea that magnetic recording is write-field limited and not demagnetization limited¹. Fundamental limitations to head field gradients give rise to a minimum transition width that is larger than the simple stability-versus-demagnetization limit². For this reason, it is highly desirable to find a magnetic head that has both large field gradient in the writing process, and a narrow width of field in the reproducing process. With this aim in mind we calculate in this paper the head field distribution of asymmetry ring heads with several inclination angles, discuss salient features of each configuration and point out the optimum conditions whereby high bit density recording can be obtained.

II. FIELD DISTRIBUTION OF AN ASYMMETRIC RING HEAD

The essence of an asymmetric ring head is shown in Fig. 1. It consists of an infinitely permeable magnetic core in a ring shape with a constant potential difference V_0 across the

air gap g which is inclined at an angle θ . The head core carries N turns of current I with magneto-motive-force NI . The head core reluctance is neglected.

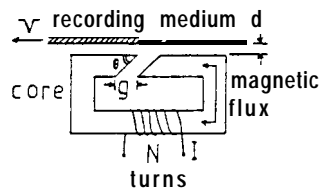


FIG. 1 Structure of an asymmetric ring head.

To obtain the head field distribution we write a generalized Schwartz-Christoffel transformation that maps a given geometry of recording head in the $Z(x,y)$ -plane onto the real axis in the complex $W(u,v)$ -plane, as shown in Fig. 2, as follows

$$\frac{dZ}{dW} = A(w + 1 - \beta)^{\frac{D-1}{D}} (W - 1 - \beta)^{\frac{1}{D}} W^{-1} \tag{1}$$

in which D is related to the inclination angle θ , β is related to the coordinate of the head corner in the W plane in relation to that in the Z -plane, and A is related to the magnifica-

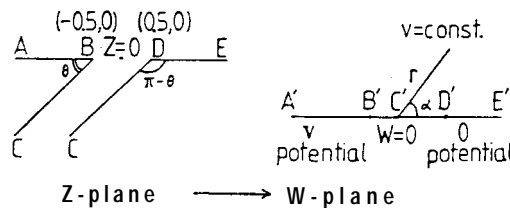


FIG. 2 Conformal mapping, from the Z -plane to the W -plane

tion (shrinkage) of the transformation itself. By means of numerical integration and the proper boundary conditions we obtain the following results:

$$\begin{aligned} \theta = 90'' & , A = 0.318 , \beta = 0 , D = 2 \\ \theta = 60'' & , A = 0.328 , \beta = 0.333 , D = 3 \\ \theta = 45'' & , A = 0.342 , \beta = 0.5 , D = 4 \\ \theta = 30'' & , A = 0.362 , \beta = 0.666 , D = 6 \\ \theta = 10'' & , A = 0.425 , \beta = 0.889 , D = 18 \end{aligned} \tag{1a}$$

For example, the point D at $(0.5, 0)$ in the Z -plane is mapped into the point D' in the W -plane at $(1, 0)$, $(1.333, 0)$, $(1.5, 0)$, $(1.667, 0)$ and $(1.889, 0)$, for $\theta = 90^\circ, 60^\circ, 45^\circ, 30''$ and $10''$ respectively, and so on. Thus, by numerical integration, we can carry out an one-to-one mapping of any point in the upper half Z -plane to a point in the W -plane, and vice versa via the inverse mapping. In the W -plane, the magnetic potential of the half line $A' C'$ is V_0 , and that of the half line $C' E'$ is 0. If we denote W by (γ, α) in the polar coordinate in the W -plane then the equipotential lines are $\alpha = \text{const.}$ The magnetic potential ψ at (γ, α) is $\frac{V_0 \alpha}{\pi}$

So,

$$\frac{\partial \psi(\gamma, \alpha)}{\partial \gamma} = 0, \frac{\partial \psi}{\partial \alpha} = \frac{V_0}{\pi} .$$

We have,

$$\begin{aligned} \frac{d\psi(W)}{dW} &= \frac{\partial \psi(\gamma, \alpha)}{\partial \gamma} / \frac{\partial W}{\partial \gamma} + \frac{\partial \psi(\gamma, \alpha)}{\partial \alpha} / \frac{\partial W}{\partial \alpha} \\ &= 0 + \frac{V_0}{\pi} / i e^{i\alpha} = - \frac{iV_0}{\pi W} \end{aligned} \quad (2)$$

If the magnetic potential in the Z-plane is $\Psi(x, y)$, the intensity of the magnetic field has components $H_x = -\frac{\partial \Psi(x,y)}{\partial x}$, $H_y = -\frac{\partial \Psi(x,y)}{\partial y}$, and

$$\begin{aligned} H_x - iH_y &= -\frac{\partial \Psi(x,y)}{\partial x} + i \frac{\partial \Psi(x,y)}{\partial y} = -\frac{d\Psi(Z)}{dZ} \\ &= -\frac{d\Psi(W)}{dW} / \frac{dZ}{dW} = \frac{iV_0}{\pi W} / \frac{dZ}{dW} \\ &= iV_0 [\pi A(W + 1 - \beta)^{\frac{D-1}{D}} (W - 1 - \beta)^{\frac{1}{D}}]^{-1} \end{aligned} \quad (3)$$

The equipotential lines are crowded near the acute corner of the head gap, and the potential correspondingly drops sharply there. Figure 3 shows essential features of the potential drop

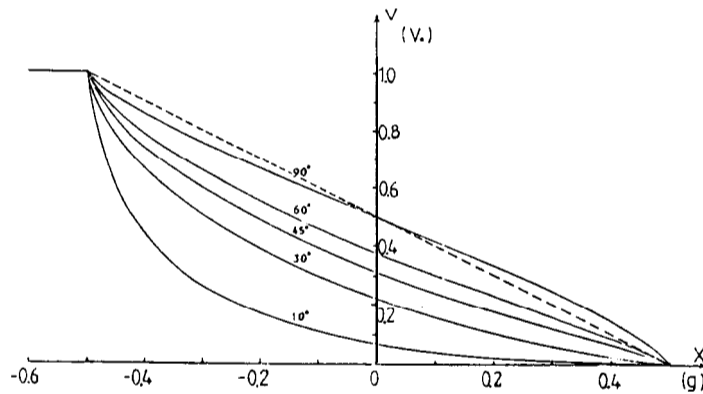


FIG. 3 Potential drop across the head gap for various θ -angles. Note the clear deviation from linearity (the dashed line) at $\theta = 90^\circ$.

across the head gap for various inclination angles θ at zero spacings. The smaller the e-angle, the sharper is the drop. Note also the clear deviation from linearity (the dashed lines) of the potential drop at $\theta = 90^\circ$. By virtue of these features the H_x component of the field dis-

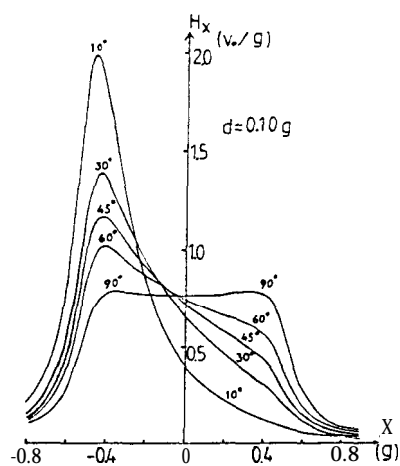


FIG. 4 The distribution of H_x field for several inclination angles, $d = 0.10$ g.

tribution is sharply peaked at low spacings. Characteristic features of the H_x field distribution at spacings $d = 0.10$ g and 0.05 g are shown in Figs. 4 and 5. The corresponding H_y fields are plotted in Figs. 6 and 7.

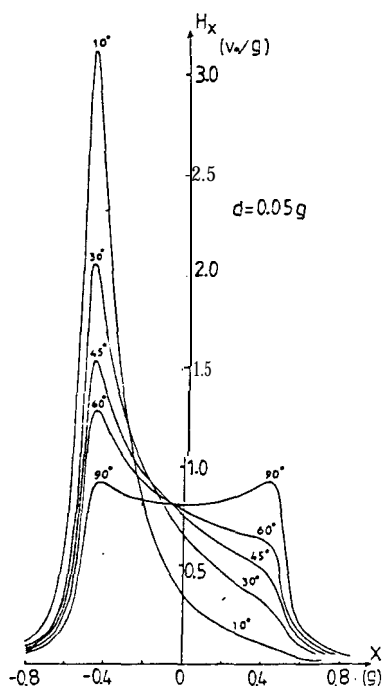


FIG. 5 The distribution of H_x field for several inclination angles, $d = 0.05$ g.

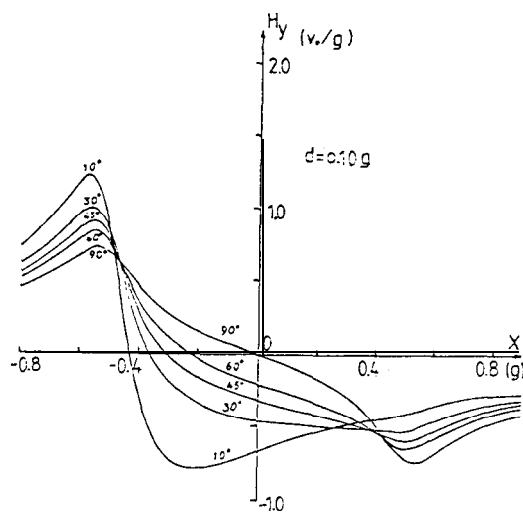


FIG. 6 The distribution of H_y field for several inclination angles, $d = 0.10$ g.

III. RECORDING PROCESSES

A. Longitudinal Mode

In the longitudinal recording mode, when the medium is traveling from right to left over the asymmetric ring head, the shape of the left edge of the H_x component field, that is, the field gradient, determines to a great extent the bit density that can be achieved. From

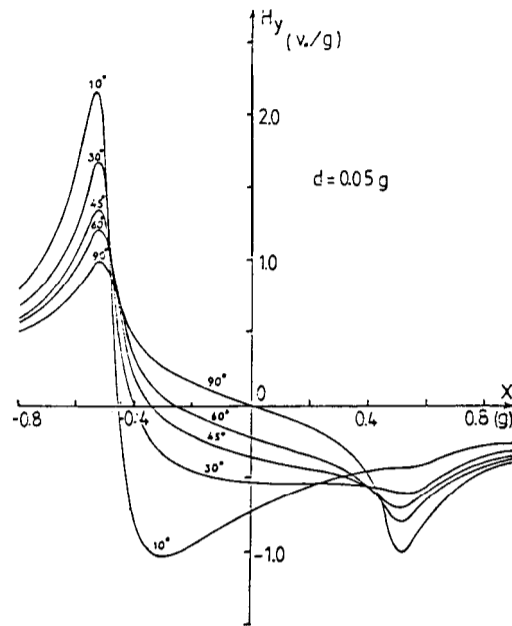


FIG. 7 The distribution of H_y field for several inclination angles, $d = 0.05g$.

the curves in Figs. 4 and 5, we obtain the field gradients (in unit of V_0/g^2) at different spacings and θ angles as shown in Table 1.

TABLE 1 The H_x field gradient at several flying heights and inclination angles. The last column contains those of a thin film head ($p = g, d = 0.2g$).

$d \backslash \theta$	90°	60°	45°	30°	10°	*
$0.15g$	2.0	2.8	3.2	4.1	5.4	2.0
$0.10g$	3.2	4.9	5.8	6.5	10.6	3.2
$0.05g$	7.0	12	15	20	30.0	7.1

* H_x field gradient values for a thin film head at a pole length equal to the gap length.

It is evident that the larger the inclination (θ small), the greater the field gradient, and the higher is the bit density that can be achieved. For comparison, the H_x component field of a thin film head³ at pole length p equal to the gap width g is shown in Fig. 8. The corresponding values of the field gradient are listed in the last column in Table 1. Clearly,

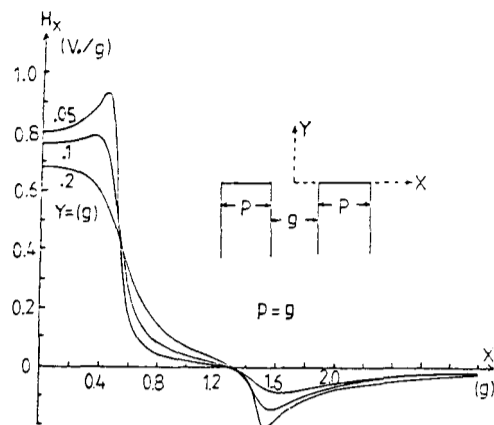


FIG. 8 The distribution of a thin film head H_x field at $p=g$, (from ref. 3).

the thin film head H_x field distribution is very similar to that of a conventional ring head ($e = 90^\circ$).

B. Perpendicular Mode

Figures 6-7 show the H_y component field at various inclination angles. The field distribution is relatively flat and broad at moderate spacings. At lower spacings, say $d = 0.05g$, the field distribution turns much more sharply, becoming applicable for perpendicular recording. When the medium is traveling from left to right, the bit density is dictated largely by the edge field gradient generated from the right side of the H_y field. The value of the field gradient is $37.5V_0/g^2$ at $\theta = 10^\circ$, $23.1V_0/g^2$ at 30° and $11.5V_0/g^2$ at 45° . Note that the field distribution dips well below zero at $\theta = 10^\circ$. This effect may well trigger magnetization reversal just recorded. The triggering field value H_y is typically about H_c . This H_y value is determined by the magnetic properties and-preparation procedures of the media concerned. We denote the extremum value of the positive (negative) portion of the head field by H_y^+ (H_y^-). The triggering field H_y ought to be substantially smaller than H_y^+ , but larger than H_y^- , in order for the system to be sound and operative. The coefficient of effectiveness of a head against the variation of the medium property can be represented by $R = (H_y^+ - H_y^-)/(H_y^+ + H_y^-)$. For different θ angles, the H_y^+ , H_y^- and R values are as shown below:

e	90°	60°	45°	30°	10°
H_y^+ (V_0/g)	0.99	1.20	1.35	1.66	2.14
H_y^- (V_0/g)	0.99	0.80	0.70	0.60	1.03
R	0	0.20	0.32	0.47	0.35

Thus an asymmetric head at $\theta \cong 30^\circ$ is better suited than at $\theta \cong 10^\circ$ for perpendicular recording.

IV. REPRODUCING PROCESS

We consider the case of longitudinal reading process. When the recording medium with an arctangent transition $M(x - x_0) = \frac{2Mr}{\pi} \tan^{-1} \frac{x - x_0}{a}$ travels over the head with a velocity $v = \frac{dx_0}{dt}$, the readback voltage $e(x_0)$ may be expressed as

$$e(x_0) \sim \int_{-\infty}^{\infty} \frac{dV(x)}{1 + (\frac{x - x_0}{a})^2} \tag{4}$$

Because the equipotential lines in the Z-plane are easily obtained by mapping the equipotential lines in the W-plane as shown in Fig. 3, the readback voltage $e(x_0)$ at different flying

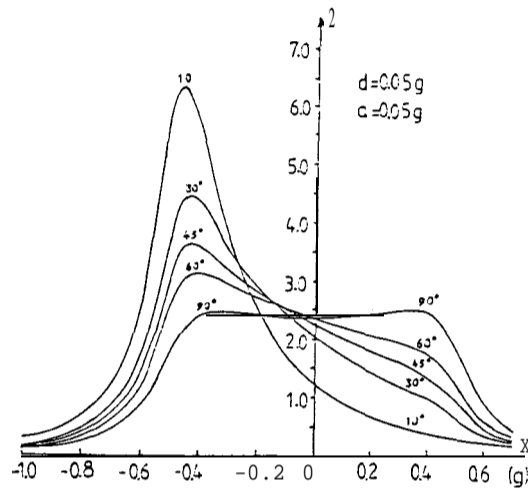


FIG. 9 Readback voltage versus θ angle at $d = 0.05g, a = 0.05g$.

heights and transition widths a can be easily calculated. Typical results are shown in Fig. 9. Numerical values at small spacing ($d = 0.05g$) for signal halfwidth (in unit of g) for different angles θ are tabulated in Table 2.

TABLE 2. Signal halfwidth versus inclination angle for different transition widths ($d = 0.05g$).

$a \backslash \theta$	90°	60°	45°	30°	10°
0.15g	1.18	1.10	0.98	0.78	0.54
0.10g	1.16	1.05	0.87	0.65	0.44
0.05g	1.10	1.01	0.07	0.53	0.32

It is apparent that the larger the inclination (smaller θ), the narrower the signal half width. Also, the smaller the transition width, the narrower the signal half width. The case for the highest resolving power is one with the minimum transition width at the smallest θ angle. The peak readback voltages are as shown in Table 3.

TABLE 3. Readback voltage versus inclination angle for different transition widths ($d = 0.05g$).

$a \backslash \theta$	90°	60°	45°	30°	10°
0.15g	2.2	2.5	2.7	3.1	3.9
0.10g	2.3	2.7	3.1	3.6	4.8
0.05g	2.5	3.2	3.7	4.5	6.4

The H_x component field of a thin film head is similar to that of the symmetric ring head, especially so within the gap region, as discussed in detail elsewhere³. The sensitivity of the head is determined by the readback peak voltage. From table 3 we see that a small value of a in combination with small θ is the best condition for high sensitivity in longitudinal mode. Table 4 summarizes the trend of the variation of the halfwidth and the peak readback voltages versus the inclination angles at $d = 0.15g$, $a = 0.10g$.

TABLE 4. Trend of signal halfwidth, peak readback voltage at different inclination angles ($d = 0.15g$, $a = 0.10g$).

θ	90°	60°	45°	30°	10°
half-width	1.22	1.14	1.04	0.90	0.65
peak-value	2.02	2.21	2.39	2.63	3.23

Clearly, the asymmetric head has better characteristics required for recording at high bit density than are possible for a symmetric head.

V. CONCLUSIONS

Head field distributions for asymmetric ring heads with several inclination angles have been calculated. It is shown that both the H_x and H_y components of field exhibit good behaviour conducive to high density recording when the inclination angle becomes large and flying height becomes small. The H_x field shows a large field gradient near the outer edge of the air gap whereas the H_y field shows a similar feature at the inner edge of the head gap. When these characteristic features are combined, one should be able to improve substantially the signal halfwidth, peak signal level and head sensitivity. The H_x field is especially suitable for longitudinal recording. For the H_y field application, high-density recording can be effectively achieved in perpendicular recording provided that the coefficient of effectiveness is properly considered so as to optimize the performance.

REFERENCE

1. J. C. Mallison and H. N. Bertram, " A Theoretical and Experimental Comparison of the Longitudinal and Vertical Modes of Magnetic Recording" . IEEE Trans. on Magnetics, Vol. MAG-20, 461-7, 1984.
2. J. E. Opfer, B.F. Spencer, B.R. Natarajan, R.A. Baugh, E.S. Murdock, C.C. Morehouse and D. J. Bromley " Thin-Film Memory Disc Development" , Hewlett-Packard Journal, Nov. 1985 pp. 4-19.
3. H. L. Huang, C. S. Wang and J. S. Yang " Fundamentals of the Recording Head Fields" , Chin. J. Phys. 25, 530-56, 1987.